JOURNAL OF AIRCRAFT
Vol. 34, No. 6, November–December 1997

Dual-Polarization Radar to Identify Drizzle, with Applications to Aircraft Icing Avoidance

Roger F. Reinking,* Sergey Y. Matrosov,† Brooks E. Martner,‡ and Robert A. Kropfli§
National Oceanic and Atmospheric Administration, Boulder, Colorado 80303

Freezing drizzle has been identified as a primary aircraft in-flight icing hazard. New evidence shows that it can be a greater hazard than freezing rain, even though the latter can be significant. Freezing drizzle may form by droplet coalescence without an intermediate melting process, so that it also can be more difficult to detect than freezing rain. Theoretical calculations of microwave scattering and verification by the initial field studies presented here demonstrate that freezing drizzle should be detectable and distinguishable from other hydrometeor types in short-wavelength, dual-polarization radar measurements of elliptical and linear depolarization ratios. A practical procedure is suggested for identifying and monitoring this aviation hazard with the radar and concurrent atmospheric temperature measurements. The WSR-88D radar (NEXRAD) has the potential to add dual-linear polarization to operationally apply this method, within certain constraints.

Introduction

CURRENT evidence indicates that supercooled droplets the size of drizzle are a primary aircraft icing hazard. The evidence is based on cloud physics measurements of freezing drizzle and associated cloud liquid–water contents quantitatively correlated with degradation in aircraft performance.[1–7] While freezing rain can certainly be a hazard, flight and wind-tunnel evidence now indicates that the hazard caused by drizzle, at least with certain aircraft or in certain circumstances, can be more serious.[5–7] For example, in freezing rain cases, a King Air research aircraft collected clear-ice coatings on the windshield, but performance degradation was not severe.[7] Also, no degradation was noted from a research flight of a Cessna Citation through freezing rain.[8] Cases with freezing drizzle, in contrast, resulted in significant increases in drag.[3,5] These, and added studies with turboprop aircraft, indicate that "freezing drizzle results in maximum rates of performance degradation while [smaller] cloud drops, [larger] freezing rain[drops] and mixed phase environments result in minor rates of performance degradation."[7]

Broadly defined, drizzle droplets have diameters between 30–500 μm, and freezing rain occurs as millimeter-size drops. Freezing rain occurs in association with warm fronts when ice particles fall through a temperature inversion, melt, and subsequently supercool. Thus, layers where freezing rain may be present can be located quite readily with temperature soundings plus radar observations of the overriding melting layer (bright band) and wind shear.[8–10] The same weather scenario can produce freezing drizzle. Here, wind shear is not necessary for the formation of freezing rain or drizzle, but it identifies the warm front interface. In contrast, wind shear is hypothesized and supported by preliminary measurements as a necessary (but not sufficient) condition for the formation of drizzle-size droplets in the absence of the melting process.[11] Wind shears may induce gravity waves that encourage broadening of the droplet size spectrum, enhancing collision and coalescence of cloud droplets to form freezing drizzle in a supercooled cloud by a process that does involve melting or a bright band.[7] Some means is needed to detect freezing drizzle thus formed, even when it occurs between layers containing ice particles, as well as when it occurs below a melting level. Also, a means is needed to differentiate and monitor transitions between freezing drizzle and freezing rain. Drizzle droplets [equivalently supercooled large droplets (SLDs), in aircraft icing terminology] were a focus of a recent Federal Aviation Administration (FAA) International Conference on Aircraft In-Flight Icing, and the development of remote-sensing methods for their detection was a consensus recommendation.[12]

Radar measurements of the depolarization ratio (DR) were made to separately identify drizzle, regular ice crystals, crystal aggregates, and graupel during the Winter Icing and Storms Project (WISP).[13] Some measurements indicating rain–drizzle distinctions were also obtained. The K_a-band (8.66-mm wavelength), Doppler, dual-polarization radar from the National Oceanic and Atmospheric Administration (NOAA) Environmental Technology Laboratory (ETL) was used.[14] This radar will detect clouds with equivalent reflectivities Z_e at least down to −30 dBZ at a 10-km range, or equivalently, ~35-μm-diam droplets in an extremely low concentration of ~0.5 cc^{-1}. Drizzle sizes are similar or much larger; concentrations for 30–50 μm sizes are generally considerably higher, for example, 100 cc^{-1} but lower at the larger sizes, for example, 0.1 cc^{-1}.[11] The tradeoffs of size and concentration make them detectable with the radar.

The objective of this paper is to demonstrate that measurements of the elliptical depolarization ratio (EDR) and linear depolarization ratio (LDR), supported by scattering calculations, provide a means to detect drizzle and differentiate it from the other hydrometeor types, to identify an aircraft icing hazard when, from supporting measurements, the drizzle is determined to be supercooled.

Background

Hydrometeors scatter microwaves according to their size, aspect ratio (shape), orientation during settling, bulk density, and the polarization state of the incident radiation. The NOAA/ETL K_a-band radar takes full advantage of this physics

Received Feb. 1, 1997; revision received May 16, 1997; accepted for publication June 18, 1997. This paper is declared a work of the U.S. Government and is not subject to copyright protection in the United States.

*Research Meteorologist, Radar Meteorology and Oceanography Division, Environmental Technology Laboratory, 325 Broadway.

†Research Physicist, Cooperative Institute for Research in Environmental Sciences, University of Colorado, Environmental Technology Laboratory, 325 Broadway.

‡Research Meteorologist, Radar Meteorology and Oceanography Division, Environmental Technology Laboratory, 325 Broadway.

§Chief, Radar Meteorology and Oceanic Division, Environmental Technology Laboratory, 325 Broadway.

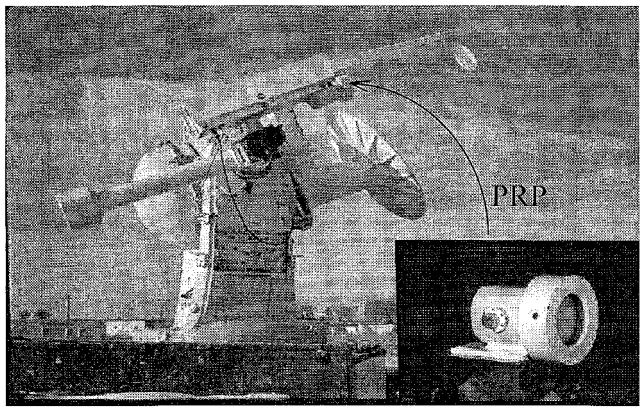

Fig. 1 NOAA ETL dual-polarization, Doppler K_a-band radar's offset Cassegrain antenna and rotatable PRP for changing the polarization state. The PRP housing is shown in the insert and on the antenna structure. The parabolic dish diameter is 1.05 m.

with an adjustable-polarization capability that is provided by a rotatable phase-retarding plate (PRP) (Fig. 1). The PRP resolves the exiting signal into two components, retards the phase of one relative to the other, and then recombines them for transmission, as described in the theory of polarized light.[15] The recombination results in circular, linear, or intermediate elliptical polarization states depending on the (adjustable) rotation angle of the PRP and on the (fixed) phase shift it induces. A linearly polarized signal is one that is transmitted with an electric field vector that remains in one plane, for example, horizontal, but varies in amplitude. For circular polarization, the amplitude is constant, but the direction rotates in a helix through space. Elliptical polarization is a compromise, with both amplitude and direction varying, depending on the degree of ellipticity. Hydrometeors modify, i.e., depolarize and backscatter these signals of each polarization state differently. One measure of the result is the depolarization ratio, DR = $10 \log(P_{co}/P_{cr})$, where P_{co} is the power returned in the radar's main channel, and P_{cr} is the power returned in cross channel, orthogonal to the transmission.

In WISP, a 79.5-deg phase-shift PRP was used, so that the radar transmitted nearly circular elliptical polarization as one extreme state, at 45-deg PRP rotation, and horizontal linear polarization as the other extreme state, at 90-deg rotation (a 90-deg phase-shift PRP would produce extremes of true circular and linear). EDR and LDR were measured. EDR was measured by transmitting fixed elliptical polarization while varying the radar's viewing angle with range-height indicator (RHI) scans from antenna elevation angle $\beta = 0$ to 175 deg. These over-the-top RHI scans smoothly move the antenna's pointing direction from one horizon, through the zenith, to near the opposite horizon in about 1 min. This viewing angle geometry is very important. Aerodynamic drag causes nonspherical hydrometeors, notably ice crystals and raindrops, to settle with preferred orientations, so that different particle types may present significantly different cross-sectional shapes to the radar when viewed from different angles. This results in depolarizations that vary measurably with β and provide a means for estimating particle types. In contrast, drizzle droplets are nearly spherical, and so the cross-sectional shape presented to the radar and, therefore, the DR does not vary with β. From the RHI scans, the differences in variation of EDR with β at constant altitude were used to determine hydrometeor type.

In a second, somewhat opposite observing mode, the radar was set at a fixed elevation angle, and the PRP was rotated at constant speed to cycle the transmitted polarization through the available continuum of states between horizontal linear and near-circular elliptical, also in about 1 min. This was repeated at two or three fixed elevation angles, for example, $\beta = 7.5$, 30, and 90 deg, and from these measurements, the limiting depolarization values LDR and EDR were used to determine hydrometeor type. With either scanning strategy, it was possible to examine data from any specific altitude.

Scattering Calculations

From Rayleigh scattering theory, calculations to differentiate among the depolarizations caused by the various pristine ice crystal types have been made and verified using measurements from the ETL K_a-band radar.[16–19] Spheres were used as a reference. The pristine ice crystals settle through the atmosphere with a preferred orientation that is random in the horizontal plane. Random deviations from this plane do occur and are specified as the standard deviation of the orientation angle from horizontal σ_θ. For $\sigma_\theta = 3$ deg, the calculated EDR-β and LDR-β relationships for the 79.5-deg phase-shift PRP are shown in Figs. 2a and 2b, respectively (as DR is defined, the sign of LDR is opposite common convention; this is convenient for the measurement methods used here). By these calculations, the EDR for planar crystals (hexagonal plates, dendrites) is predicted to decrease by about 9 ± 2 dB as β is increased from 0 to 90 deg. The pattern is the same, but the magnitude of change with β is much less for the columnar crystal types. Overall, the EDR for the various crystals is offset from the β-invariant -14.8 dB signature for spheres (drizzle) by 2–10 dB at elevation angles nearest the horizon, and less near zenith. With linear polarization transmitted, the LDR for drizzle is expected to be about $+35$ dB, a limiting value for this radar. The offset of drizzle from depolarizations caused by the planar ice crystals is of the same order as that in EDR and, likewise, large (8 ± 2 dB) at low β. The DR-β curve slopes are opposite for columnar and planar crystals in LDR (Fig. 2b) but the same in EDR, for the 79.5-deg PRP (Fig. 2a). Consequently, in LDR, the columnar crystal depolarizations theoretically increase with increasing β, with the result that the predicted maximum offset from drizzle is much larger (11–19 dB) than that in EDR and occurs toward zenith rather than low β.

Figures 2a and 2b show that radar measurements of EDR or LDR as a function of β should differentiate columnar from planar crystal types and those from drizzle. The differentiation might be easiest in LDR because of 1) the larger differences in DR among particle types and 2) the opposite slopes of the DR-β curves for columnar vs planar crystals. This would be true if not for 3) the effect of σ_θ. The estimation of ice particle type is degraded only slightly by randomness in crystal orientation using near-circular EDR but substantially using LDR; i.e., LDR depends most heavily on σ_θ.[16] The calculations in Figs. 2a and 2b are based on $\sigma_\theta = 3$ deg; at least this much randomness is expected in snow crystals. The effect of a more random orientation, for example, $\sigma_\theta = 10$ deg, is that the LDR-β curves for columnar crystals become clustered with those for planar crystals through a narrowed dynamic range and widened range of elevation angles, such that practical differentiation decreases significantly (Fig. 2c vs 2a). Measurements confirm that the columnar and planar crystal types can be better differentiated using EDR rather than LDR, perhaps because of the orientation effect.[18,19] However, the model results in Fig. 2c also predict that the separability in LDR of both columnar and planar habits from drizzle ($+35$ dB) will increase measurably, by 3–5 dB, with an increase in σ_θ from 3 to 10 deg.

Drizzle droplets and raindrops have a bulk density of 1 g cm^{-3}, that of pristine ice is less and that of aggregates is much less, resulting in differences in microwave scattering and depolarization. Also, shape is still a key factor. Droplet shape can be related to an equivalent diameter D_0, the diameter of a sphere of the same volume as the deformed drop. Laboratory experiments have defined the relationship of D_0 to aspect ratio, a/b, where a and b are the minor and major axes, respectively.[20–22] Cloud and drizzle droplets falling at terminal velocity remain perfect spheres when $D_0 \leq 280$ μm. Droplets of 280 μm $\leq D_0 \leq 1$ mm resemble slightly deformed oblate spheroids; a/b is 0.996 for 500-μm droplets, confirming that

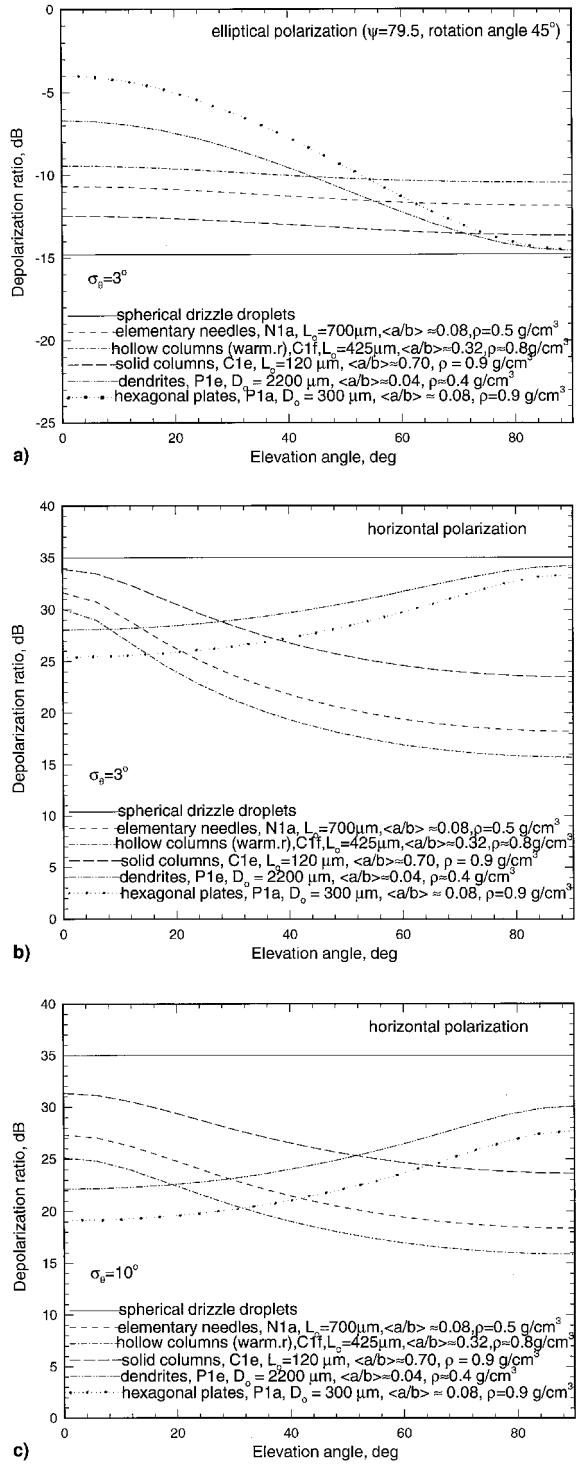

Fig. 2 Calculations of the depolarization ratio, DR (dB), as a function of radar elevation angle, β (deg), for various regular ice crystals and drizzle: a) EDR for a 79.5-deg phase shift and σ_θ = 3 deg, b) LDR, σ_θ = 3 deg; and c) LDR, σ_θ = 10 deg. Depolarization increases as the absolute value of DR decreases toward zero (after Ref. 19).

drizzle is nearly spherical and should not measurably depolarize incident radiation. For small to medium-sized raindrops with D_0 of 0.8, 1.0, and 1.5 mm, respectively, a/b is approximately 0.98, 0.97, and 0.94. With the increasing nonsphericity, an elliptically (or circularly) polarized signal will be increasingly depolarized. Raindrops falling at terminal velocities are expected to remain predominantly oblate.[23,24] Near D_0 = 2.8 mm, $a/b \approx 0.85$, raindrops develop flattened bases,[21,22] and the depolarization will be substantial when the incident radiation

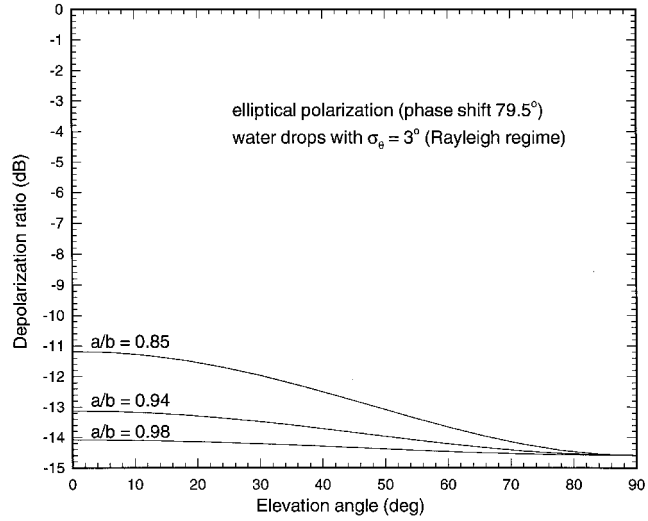

Fig. 3 Calculations of EDR (dB) for monodispersed drops of D_0 = 0.8, 1.5, and 2.8 mm, for which $a/b \approx$ 0.98, 0.94, and 0.85, respectively. Rayleigh scattering is assumed in these first-order approximations, although it is not strictly applicable to the larger drops.

is elliptically or circularly polarized. However, a linear signal polarized in the horizontal plane will not see the nonsphericity and will not be depolarized unless the raindrops deviate from a horizontal settling orientation; then the differentiation between drizzle and rain is expected to be possible, but still difficult using a horizontal LDR. Rigorous calculations have not yet been made, but depolarizations of an elliptical signal transmitted with a 79.5-deg phase shift are approximated in Fig. 3 for some of the drop sizes noted in the preceding text (here monodispersed drops are assumed, whereas realistic hydrometeor-size distributions were used for the calculations in Figs. 2a–2c). For consistency with Figs. 2a and 2b, σ_θ = 3 deg is assumed. This small value of σ_θ seems reasonable because mean raindrop canting angles of ~0.5–1.4 deg, with standard deviations of ~2 deg and maximum deviations of ~5 deg, have been estimated from a few measurements and theory.[25,26] Figure 3 indicates that 0.8-mm drops ($a/b \approx 0.98$) will appear spherical at zenith and produce an increment of depolarization of about 0.5 dB at β = 10 deg. The effect of this nonsphericity may be marginally measurable and distinguishable from spherical 500-μm drizzle. A 1.5-mm drop with a/b = 0.94 should produce a detectable increment of depolarization of about 1.5 dB for β = 10 vs 90 deg. Still larger drops enter the Mie scattering regime for K_a-band radar; these first-order Rayleigh approximations suggest that a 2.8-mm drop would depolarize the signal substantially, incrementally about 3.3 dB at β = 10 deg, relative to 90 deg.

To summarize, these scattering calculations predict that EDR will provide a very good capability to differentiate among crystals of the various habits, to distinguish these from drizzle, and possibly drizzle ($D_0 \leq$ 500 μm) from rain. However, if the objective is limited to distinguishing drizzle from ice hydrometeors, LDR should offer a good alternative. With either polarization, if the liquid hydrometeors are then determined to be supercooled, an icing situation would be identified.

Measurements

Radar measurements with in situ particle sampling have verified many of the calculations for ice crystals in Fig. 2.[17–19] For example, during WISP, many stratiform clouds such as that indicated by the radar reflectivity factor Z_e, in Fig. 4a, produced planar crystals. The EDR measured in RHI scans through these crystals (Fig. 4b), which were persistent and dominant throughout the cloud volume, provided excellent fits to the theory (Fig. 5), and the differentiation from signatures

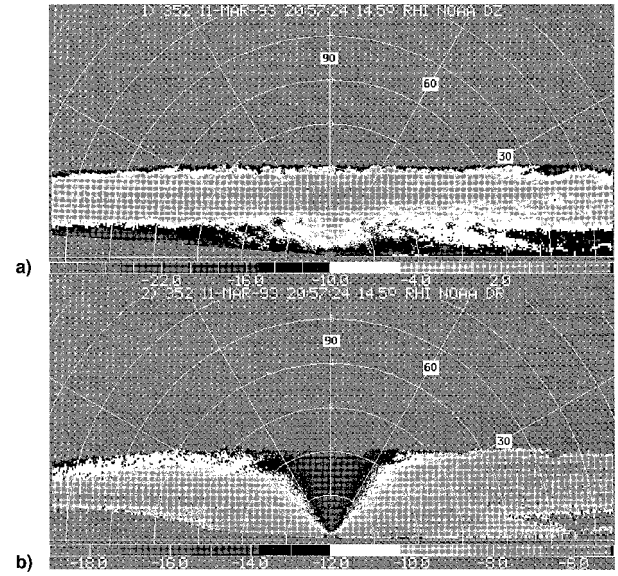

Fig. 4 a) Radar reflectivity Z_e (dBZ), from an over-the-top RHI scan (horizon-to-horizon through zenith) through a stratiform cloud that was producing planar dendritic snow crystals (1-km range rings, 2057 UTC 11 March 1993) and b) distinctive EDR (dB) signature from the planar dendritic snow crystals falling from the cloud volume. Gray scales of Z_e and EDR are indicated at the base of each frame.

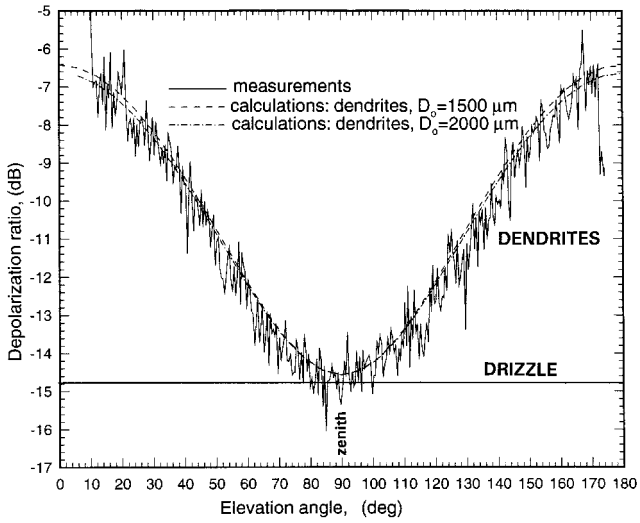

Fig. 5 Measured EDR-β curve from a constant-altitude plane (~1 km AGL) in Fig. 4b, with theoretical EDR-β curves for dendrites and drizzle (after Ref. 19).

expected from drizzle was lucid (Figs. 2a and 5). The distinctive variation of EDR with radar elevation angle β in Fig. 4b would have been replaced with ~−14.8 dB uniformly at all β, if drizzle had instead been present. In contrast are RHI scans through a cloud system producing drizzle and light rain, at 2114 and 2209 Coordinated Universal Time (UTC) 6 April 1993. Figures 6a and 7a show Z_e; Figs. 6b and 7b show EDR. In each scan, the melting layer is evident as a dark band (technically the bright band) in EDR, and in more subtle discontinuities in Z_e. In this system, the precipitation falling below the melting layer did not subsequently supercool, but that does not affect this demonstration that drizzle can be detected and differentiated from rain, such that a determination of supercooling would identify freezing drizzle or rain. The precipitation was light; primarily, $Z_e \approx 0$–20 dBZ. In the two scans, EDR at all elevation angles was more negative than −12.5 dB, thus establishing a clear separation from the EDR of ice crystals like

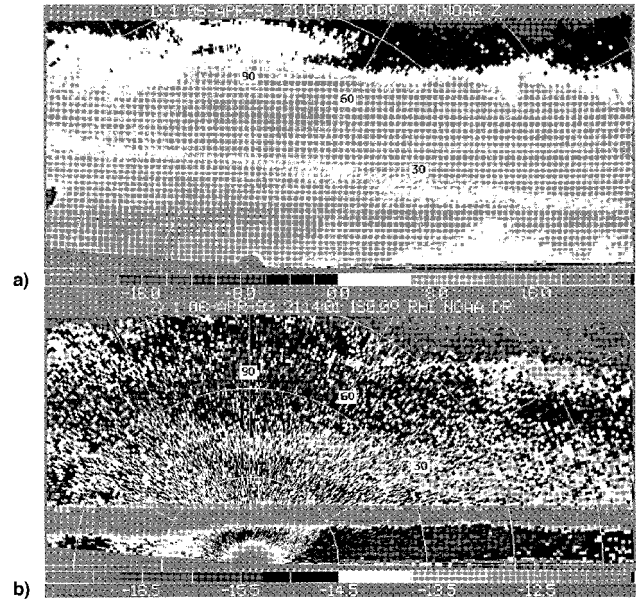

Fig. 6 Over-the-top RHI scans of a) Z_e (dBZ) and b) EDR (dB) in drizzle and light rain (1-km range rings; 2114 UTC 6 April 1993). Gray scales are at base of frames.

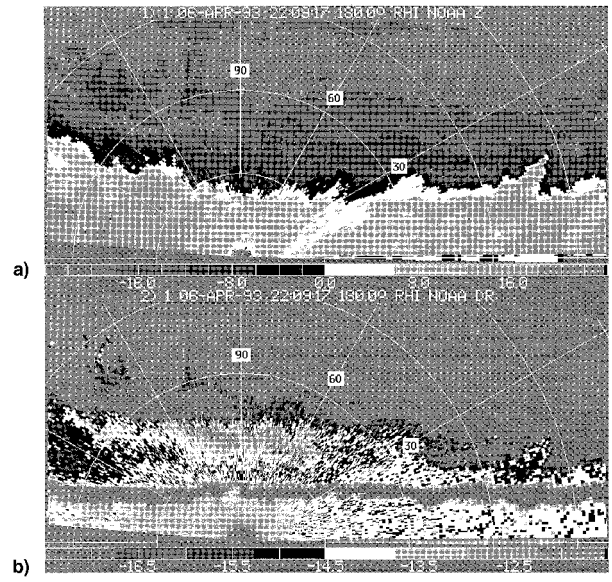

Fig. 7 Over-the-top RHI scans in light rain, from 2209 UTC 6 April 1993, as in Fig. 6.

those represented in Figs. 4b and 5. Considerable differences in EDR are evident between the two scans, and some horizontal gradients can be noted. Figure 6b shows a large, dark area below $\beta \approx 25$ deg, where EDR < −14.5 dB and, according to the theory, drizzle-size droplets were definitely present. In contrast, in a zone at close range over the radar, between $\beta \approx 30$–175 deg, much of the signal is in the range of $-14.5 \leq$ EDR ≤ -13.5 dB, indicating drops larger than drizzle. This zone is approximately the same as the area of highest reflectivities and precipitation rate in Fig. 6a, although a one-to-one correlation between EDR and Z_e should not be expected and does not occur. Recorded comments indicated very light, very small drop rain at the ground at the radar site. Larger reflectivities were not measured at the later time (Fig. 7a), but drops larger than drizzle are suggested by depolarizations in the range of $-14.5 \leq$ EDR ≤ -12.8 dB (Fig. 7b). The log book record indicated largest drops of 2 mm on a glass surface; largest equivalent spheres would have diameters of the order of 1.5 mm.

These depolarizations from drizzle and light rain are more precisely indicated in Fig. 8 where the values of EDR as a function of β are presented for a 0.30-km above ground level (AGL) constant-altitude transect through each RHI. The solid experimental curve is from the scan at 2114 UTC (Fig. 6b). Here, EDR closely approximates the −14.8 dB theoretical value for spherical drizzle ($D_0 \leq 500$ μm) between a β = 5 and 25 deg. From β = 30 to 90 deg to 175 deg, the smoothed EDR-β curve defined by the experimental values is not as flat and near −14.8 dB as it would be for droplets with $D_0 \leq 500$ μm; rather, it is slightly concave upward with EDR ≈ −14.3 dB at β = 30 and 150 deg, and EDR ≈ −14.7 dB at β = 90 deg. By the approximated theory in Fig. 3, this suggests a drop axis ratio, $a/b \approx 0.98$, and a $D_0 \approx 800$ μm; the best fit occurs between β = 100 and 170 deg. Still larger drops are suggested between β = 45 and 90 deg, where fit of the smoothed curve to the data is not as good. These data suggest that depolarizations caused by the nonsphericity of drops only a few hundred microns larger than drizzle are indeed differentiable from the signature of drizzle. The imagery (Fig. 6b) better illustrates the area with drizzle (the dark area below β ≈ 30 deg and below the melting layer), while this EDR-β curve more precisely quantifies the signal.

In comparison, in the dotted EDR-β curve in Fig. 8, from 0.30 km AGL in the 2209 UTC scan (Fig. 7b), EDR varies mainly between −13.0 and −13.8 dB. These depolarizations are measurably greater (nearer to zero decibels) than any of those for 2114 UTC and indicate drops larger than drizzle across the entire scan. This EDR-β curve does not behave according to the theory in Fig. 3; this suggests large drops of variable size across the scan, drops large enough to have more significant orientation effects and/or drops beyond the upper size limits of the K_a-band Rayleigh regime ($D_0 \approx 1$–2 mm). At least the differentiation of the rain from the drizzle is obvious.

The RHI scans provided measurements of EDR but not LDR. From PRP rotations at fixed antenna elevation angles in drizzle, dendrites, and graupel, EDR and LDR were measured concurrently as extreme values. For drizzle (Fig. 9a), LDR = +34.6 ± 0.9 dB and EDR = −14.7 ± 0.5 dB; these nearly matched calculated values of +35 and −14.8 dB, respectively. This PRP rotation was at β = 30 deg, but the measured values were quite independent of elevation angle, as expected for drizzle. In contrast, for dendrites (planar crystals, Fig. 9b), LDR = +24 ± 3 dB and EDR = −8.6 ± 0.3 dB at β = 30 deg, and the depolarizations depended on β, as in Figs. 2a and 2b, for an additional definitive and theoretically verifiable differentiation from drizzle. Aggregates, of dendrites for example, introduce some uncertainties in specific differentiation, but show a β dependency distinguishing them from drizzle.[17] In clouds with mixed hydrometeor types, dominance determines the depolarization.[19] Because of the liquid-to-ice vapor pressure gradient, if drizzle is not dominant, it will tend to be consumed by ice particles, to diminish any icing hazard.[7]

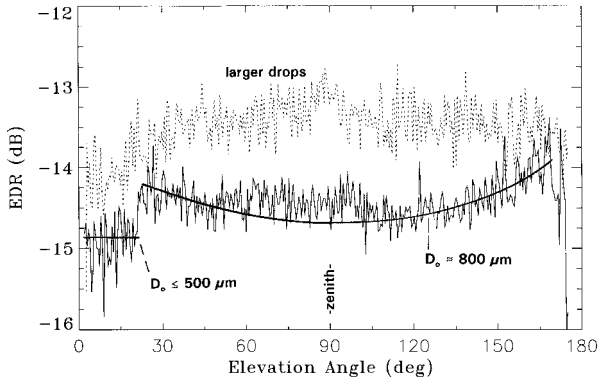

Fig. 8 EDR (dB) as function of β for an altitude of 0.30 km AGL, for 2114 UTC (solid) and 2209 UTC (dotted), from the RHI scans in Figs. 5b and 6b. Smoothed curves compared to scattering calculations suggest drop sizes.

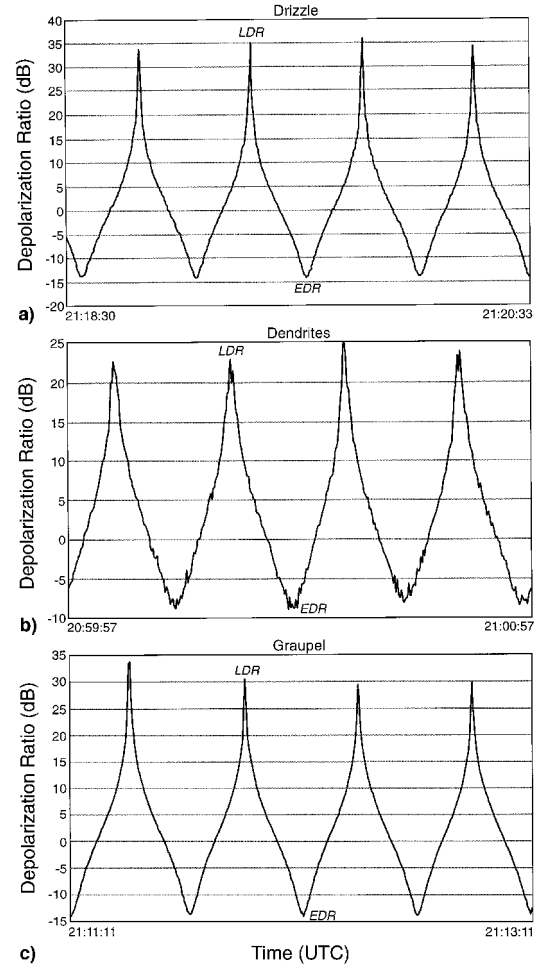

Fig. 9 DR vs time from one-cycle PRP rotations. Positive maxima are LDR (dB); negative minima are EDR (dB); peak-to-peak = 90-deg rotation: a) in drizzle, β = 30 deg, 0.50-km range, 0.25 km AGL, 6 April 1993; b) in planar crystals (dendrites), β = 30 deg, 2-km range, 1 km AGL, 11 March 1993; and c) in graupel, β = 90 deg, 1-km range, 1 km AGL, 8 February 1994. Varied ordinate scale reflects the differences in depolarization.

Graupel is the ice hydrometeor that is most similar in shape to drizzle. Therefore, although graupel and freezing drizzle normally occur in atmospheres with mutually exclusive temperature soundings (graupel in convective clouds and drizzle in stratiform clouds), a capability to differentiate them would establish considerable confidence for distinguishing drizzle from any ice hydrometeor. No K_a-band scattering calculations have been made for graupel. However, in previously reported measurements of EDR using the 79.5-deg PRP, graupel particles depolarized the signal 1–2 dB more than drizzle and slightly larger drops.[18,19] Graupel or possibly crystal aggregates are indicated in the EDR signatures at altitudes above the melting layer in Figs. 6b and 7b, and distinctions from the drizzle and light rain below the melting layer are evident. PRP rotations in graupel (Fig. 9c) showed consistent departures from the EDR for drizzle, with little EDR variation with β, similar to those previously reported. With EDR = −13.8 ± 0.3 dB and LDR = +32.1 ± 4.6 dB, the average departure from drizzle values in LDR (~3.9 dB) was notably larger (although more erratic) than in EDR (~1 dB). These results are very encouraging for the general application of the depolarization measurements to identify the drizzle.

Hypothesized Procedure for Routine Detection of Freezing Drizzle

The scattering calculations and initial measurements show that depolarization can be used to identify drizzle. With a conjunctive determination that the drizzle is supercooled, freezing drizzle should be identifiable. In a simplified overview, a procedure that could be transformed into an operational algorithm would include the following elements. The radar reflectivity measurements would simply determine cloud and precipitation boundaries to constrain the altitudes that have any possibility of producing freezing drizzle. The measurement of depolarization as a function of radar elevation angle and altitude, in concert with supporting theoretical calculations, for example, Figs. 2a–2c and Fig. 3, would then isolate layers with drizzle from other parts of a cloud. The measurements of DR, for example, EDR or LDR, from either RHI scans or PRP rotations should achieve the desired drizzle detection. Stepwise, the procedure would be as follows:

1) Make an over-the-top RHI scan, or conduct PRP rotations at more than one elevation angle including 90 deg.

2) Examine the vertical profile of DR; at 90-deg elevation, layers with low DR could be either drizzle drops, raindrops, or plate crystals, but not column crystals.

3) Examine the variation of DR with elevation angle at the altitude of each layer with low DR; if DR is independent of elevation angle, drizzle is indicated.

4) Reinforce this determination of the presence and altitude of freezing drizzle with supplemental measurements.

Temperature profiles to define altitudes of supercooling are the highest-priority supplement. These would best be obtained continuously, as with a radio-acoustic sounding system (RASS), although frequent rawinsondes would be helpful. Other measurements are not required, but would strengthen the technology. Continuous microwave radiometer measurements would predetermine the absence or presence as well as the vertically integrated quantity of liquid water[27] but not the form (small cloud droplets, drizzle, or rain), which is left to the radar. Newer technologies use ensembles of remote sensors to profile cloud liquid water, for example, a cloud-sensing radar, RASS, microwave radiometer, and ceilometer.[27,28] Without added instruments, a vertical velocity measurement with the Doppler radar would help to discriminate drizzle from rain via differences in terminal velocity if air motion is accounted for; and high-angle, conical scans would provide high-resolution wind profiles to identify any cloud layer where wind shear might be promoting coalescence to form supercooled drizzle drops above or in the absence of a melting layer.

Conclusions

To be effective in the detection, prediction, and warning of freezing drizzle (equivalently, SLDs), remote-sensing methods need to characterize the SLD environment and directly detect these droplets. Microwave-scattering calculations and initial measurements with the NOAA/ETL K_a-band (8.66 mm) cloud-sensing radar indicate that direct detection and differentiation of freezing drizzle from ice hydrometeors and freezing rain can be accomplished with dual-polarization measurements accompanied by temperature profiling. The detectability by radar is a function of the polarization state of the transmitted signal. In this study, measurement of the depolarization by hydrometeors of elliptically polarized transmitted radiation was effective in separately identifying drizzle, ice crystals, and rain. A still better isolation is possible from true circular polarization that would increase the dynamic range of depolarization signatures to achieve the widest separation of the various individual hydrometeor types, including that of drizzle from rain; this is readily feasible with a phase-retarding plate that induces the necessary 90-deg phase shift in the transmitted signal.

The depolarization produced by the interaction of the hydrometeors with transmitted horizontal linear polarization is less well behaved in distinguishing among the ice hydrometeor types but is theoretically predicted to do well in differentiating drizzle from the ice hydrometeors. The preliminary measurements support this prediction. The differentiation of drizzle and rain with horizontal linear polarization is problematic. This distinction should be more measurable with a nonhorizontal linear polarization that is transmitted at a substantial angle from horizontal to take advantage of the nonsphericity of flattened raindrops.

Important supporting measurements can be provided by the radar itself and other instrumentation. High radar resolution through the vertical extent of a cloud and reasonable cloud uniformity over about 10 km horizontally are important to the success of this technology. The range of detection may therefore be limited to the locale of the radar, for example, the vicinity of an airport; 12.5 or 25 km radar ranges were used in these studies. The preliminary K_a-band calculations of depolarization by rain-sized drops can be improved with the use of realistic drop-size distributions, with consideration for Mie as well as Rayleigh scattering. With testing to confirm the hypothesized drizzle detection procedure, transfer to operations may become possible, and adaptations of existing radars obviously offer significant cost advantages. The WSR-88D radar (NEXRAD) presently transmits and receives single horizontal polarization but is engineered to be retrofitted for dual-linear polarization. Thus, given that (freezing) drizzle is detectable in LDR, technology transfer to NEXRAD may be possible without a major capital investment. A linear polarization transmitted with an orientation at 45 deg relative to horizontal, for example, would enhance the capability. Certain constraints apply to the WSR-88D; the high sensitivity of these radars is compromised by much poorer resolution, more serious ground clutter problems, and the longer wavelength (10 cm, S-band) than those of the K_a-band radar. Also, the present operational scanning modes do not include high antenna elevation angles or RHI scans, although the hardware is capable of doing this. Even with such constraints, the dual-polarization capability of the WSR-88D for detecting drizzle-sized droplets should be tried.

In summation, the combination of the theoretical calculations and measurements demonstrate a realistic potential for differentiating freezing drizzle from ice hydrometeors and freezing rain with dual-polarization radar and supporting atmospheric measurements.

Acknowledgments

The data for this work were collected during WISP under the FAA's Aviation Weather Development Program through a subcontract with the National Center for Atmospheric Research. Roy Rasmussen and Marcia Politovich directed WISP. Michelle Ryan provided data processing support. Bruce Bartram and Kurt Clark engineered and operated the radar and received a NOAA Bronze Medal for their innovations.

References

[1]Cooper, W. A., Sand, W. R., Politovich, M. K., and Veal, D. L., "Effects of Icing on Performance of a Research Airplane," *Journal of Aircraft*, Vol. 21, No. 9, 1984, pp. 708–715.

[2]Sand, W. R., Cooper, W. A., Politovich, M. K., and Veal, D. L., "Icing Conditions Encountered by a Research Aircraft," *Journal of Climate and Applied Meteorology*, Vol. 23, No. 10, 1984, pp. 1427–1440.

[3]Politovich, M. K., "Aircraft Icing Caused by Large Supercooled Droplets," *Journal of Applied Meteorology*, Vol. 28, No. 9, 1989, pp. 856–868.

[4]Cober, S. G., Isaac, G. A., and Strapp, J. W., "Aircraft Icing Measurements in East Coast Winter Storms," *Journal of Applied Meteorology*, Vol. 34, No. 1, 1995, pp. 88–100.

[5]Politovich, M. K., "Response of a Research Aircraft to Icing and Evaluation of Severity Indices," *Journal of Aircraft*, Vol. 33, No. 2, 1996, pp. 291–297.

[6]Ashendon, R., Lindberg, W., Marwitz, J., and Hoxie, B., "Airfoil

Performance Degradation by Supercooled Cloud, Drizzle, and Rain Drop Icing," *Journal of Aircraft*, Vol. 33, No. 6, 1996, pp. 1040–1046.

[7]Ashenden, R., and Marwitz, J. D., "Turboprop Aircraft Performance Response to Various Environmental Conditions," *Journal of Aircraft*, Vol. 34, No. 3, 1997, pp. 278–287.

[8]Prater, E. T., and Borho, A. A., "Doppler Radar Wind and Reflectivity Signatures with Overrunning and Freezing-Rain Episodes: Preliminary Results," *Journal of Applied Meteorology*, Vol. 31, No. 11, 1992, pp. 1350–1358.

[9]Martner, B. E., Snider, J. B., Zamora, R. J., Byrd, G. P., Nizoil, T. A., and Joe, P. I., "A Remote Sensing View of a Freezing Rain Storm," *Monthly Weather Review*, Vol. 121, No. 9, 1993, pp. 2562–2577.

[10]Reinking, R. F., Caiazza, R., Kropfli, R. A., Orr, B. W., Martner, B. E., Niziol, T. A., Byrd, G. P., Penc, R. S., Zamora, R. J., Snider, J. B., Ballentine, R. J., Stamm, A. J., Bedford, C. D., Joe, P. I., and Koscielny, A., "The Lake Ontario Winter Storm (LOWS) Project," *Bulletin of the American Meteorological Society*, Vol. 74, No. 10, 1993, pp. 1828–1849.

[11]Pobanz, B. M., Marwitz, J. D., and Politovich, M. K., "Conditions Associated with Large-Drop Regions," *Journal of Applied Meteorology,* Vol. 33, No. 11, 1994, pp. 1366–1372.

[12]Riley, J., and Horn, B. (eds.), *Proceedings of the FAA International Conference on Aircraft In-Flight Icing, Plenary Sessions*, Vol. 1, National Technical Information Service, Springfield, VA, DOT/FAA/AR-96/81, 1996.

[13]Rasmussen, R., Politovich, M., Marwitz, J., Sand, W., McGinley, J., Smart, J., Pielke, R., Rutledge, S., Wesley, D., Stossmeister, G., Benstein, B., Elmore, K., Powell, N., Westwater, E., Stankov, B. B., and Burrows, D., "Winter Icing and Storms Project (WISP)," *Bulletin of the American Meteorological Society*, Vol. 73, No. 8, 1992, pp. 951–974.

[14]Kropfli, R. A., Matrosov, S. Y., Uttal, T., Orr, B. W., Frisch, A. S., Clark, K. A., Bartram, B. A., Reinking, R. F., Snider, J. B., and Martner, B. E., "Cloud Physics Studies with 8-mm-Wavelength Radar," *Atmospheric Research*, Vol. 35, Nos. 2–4, 1995, pp. 299–313.

[15]Shurcliff, W. A., *Polarized Light*, Harvard Univ. Press, Cambridge, MA, 1962.

[16]Matrosov, S. Y., "Theoretical Study of Radar Polarization Parameters Obtained from Cirrus Clouds," *Journal of the Atmospheric Sciences*, Vol. 48, No. 8, 1991, pp. 1062–1070.

[17]Matrosov, S. Y., Reinking, R. F., Kropfli, R. A., and Bartram, B. W., "Estimation of Ice Hydrometeor Types and Shapes from Radar Polarization Measurements," *Journal of Atmospheric and Oceanic Technology*, Vol. 13, Feb. 1996, pp. 85–96.

[18]Reinking, R. F., Matrosov, S. Y., and Bruintjes, R. T., "Hydrometeor Identification with Elliptical Polarization Radar: Applications to Glaciogenic Cloud Seeding," *Journal of Weather Modification*, Vol. 28, No. 1, 1996, pp. 6–18.

[19]Reinking, R. F., Matrosov, S. Y., Bruintjes, R. T., and Martner, B. E., "Identification of Hydrometeors with Elliptical and Linear Polarization K_a-band Radar," *Journal of Applied Meteorology*, Vol. 36, No. 4, 1997, pp. 322–339.

[20]Pruppacher, H. R., and Beard, K. V., "A Wind Tunnel Investigation of the Internal Circulation and Shape of Water Drops Falling at Terminal Velocity in Air," *Quarterly Journal of the Royal Meteorological Society*, Vol. 96, No. 408, 1970, pp. 247–256.

[21]Pruppacher, H. R., and Pitter, R. L., "A Semi-Empirical Determination of the Shape of Cloud and Rain Drops," *Journal of the Atmospheric Sciences,* Vol. 28, No. 1, 1971, pp. 86–94.

[22]Pruppacher, H. R., and Klett, J. D., *Microphysics of Clouds and Precipitation,* D. Reidel, Boston, MA, 1978, pp. 311–322.

[23]Hall, M. P. M., Goddard, J. W. F., and Cherry, S. M., "Identification of Hydrometeors and Other Targets by Dual-Polarization Radar," *Radio Science*, Vol. 19, No. 1, 1984, pp. 37–50.

[24]Seliga, T. A., Bringi, V. N., and Al-Khatib, H. H., "A Preliminary Study of Comparative Measurements of Rainfall Using the Differential Reflectivity Radar Technique and a Raingage Network," *Journal of Applied Meteorology*, Vol. 20, No. 11, 1981, pp. 1362–1368.

[25]McCormick, G. C., and Hendry, A., "Polarization Properties of Transmission Through Precipitation over a Communication Link," *Journal de Researches Atmospherique*, Vol. 8, Nos. 1–2, 1974, pp. 175–187.

[26]Beard, K. V., and Jameson, A. R., "Raindrop Canting," *Journal of the Atmospheric Sciences*, Vol. 44, No. 2, 1983, pp. 448–454.

[27]Stankov, B. B., and Bedard, A. J., Jr., "Remote Sensing Observations of Winter Aircraft Icing Conditions: A Case Study," *Journal of Aircraft*, Vol. 31, No. 1, 1994, pp. 79–89.

[28]Politovich, M. K., Stankov, B. B., and Martner, B. E., "Determination of Liquid Water Altitudes Using Combined Remote Sensors," *Journal of Applied Meteorology*, Vol. 34, No. 9, 1995, pp. 2060–2075.